

1-1-2012

Asymmetric cryorolling for fabrication of nanostructural aluminum sheets

Hailiang Yu

University of Wollongong, hailiang@uow.edu.au

Cheng Lu

University of Wollongong, chenglu@uow.edu.au

K. Tieu

University of Wollongong, ktieu@uow.edu.au

Xianghua Liu

Northeastern University China, liuxh@uow.edu.au

Yong Sun

University of Wollongong, ys994@uowmail.edu.au

See next page for additional authors

Follow this and additional works at: <https://ro.uow.edu.au/engpapers>



Part of the [Engineering Commons](#)

<https://ro.uow.edu.au/engpapers/5187>

Recommended Citation

Yu, Hailiang; Lu, Cheng; Tieu, K.; Liu, Xianghua; Sun, Yong; YU, Qingbo; and Kong, Charlie: Asymmetric cryorolling for fabrication of nanostructural aluminum sheets 2012, 1-5.

<https://ro.uow.edu.au/engpapers/5187>

Authors

Hailiang Yu, Cheng Lu, K. Tieu, Xianghua Liu, Yong Sun, Qingbo YU, and Charlie Kong



Asymmetric cryorolling for fabrication of nanostructural aluminum sheets

Hailiang YU^{1,2}, Cheng LU¹, Kiet TIEU¹, Xianghua LIU³, Yong SUN¹, Qingbo YU³ & Charlie KONG⁴

¹School of Mechanical, Materials & Mechatronic Engineering, University of Wollongong, NSW 2500, Australia, ²School of Mechanical Engineering, Shenyang University, Shenyang 110044, China, ³State Key Laboratory of Rolling and Automation, Northeastern University, Shenyang 110004, China, ⁴Electron Microscope Unit, University of New South Wales, Sydney, NSW 2250, Australia.

SUBJECT AREAS:
APPLIED PHYSICS
MECHANICAL PROPERTIES
NANOSCALE MATERIALS
METALS AND ALLOYS

Received
21 July 2012

Accepted
1 October 2012

Published
25 October 2012

Correspondence and
requests for materials
should be addressed to
H.Y.
(yuhailiang1980@
tom.com; hailiang@
uow.edu.au)

Nanostructural Al 1050 sheets were produced using a novel method of asymmetric cryorolling under ratios of upper and down rolling velocities (RUDV) of 1.1, 1.2, 1.3, and 1.4. Sheets were rolled to about 0.17 mm from 1.5 mm. Both the strength and ductility of Al 1050 sheets increase with RUDVs. Tensile strength of Al sheets with the RUDV 1.4 is larger 22.3% of that for RUDV 1.1, which is 196 MPa. The TEM observations show the grain size is 360 nm when the RUDV is 1.1, and 211 nm for RUDV 1.4.

In recent years, a lot of interest has been shown in the production of materials with nano-sized grains, especially in bulk through Severe Plastic Deformation (SPD) techniques. This interest is due to unique physical and mechanical properties inherent to various nanostructural materials. The SPD techniques, which include high-pressure torsion¹, reciprocal extrusion², equal-channel angular pressing (ECAP)³, accumulative roll bonding^{4,5}, repetitive corrugation and straightening⁶, constrained groove pressing⁷, equal channel rolling⁸, asymmetric rolling, cryorolling, etc, have been developed to fabricate bulk nanostructural or ultrafine grain samples of different metals. Compared with above SPD techniques, the asymmetric rolling and cryorolling employed have potential for large-scale industrial applications of nanostructural materials.

In asymmetric rolling, sheets are rolled between rolls that either are of different diameters, or are rotating at different velocities. Asymmetric rolling has a potential for industrial applications because it involves a decrease in the rolling pressure and torque and an improvement of the rolled strip shape^{9,10}. In addition, it is generally claimed that during asymmetric rolling, the complete strain state imposed on the strip is a combination of plane strain deformation and of an additional shear component imposed on the rolling plane in the rolling direction^{11,12}. Several studies have shown that this additional shear strain contributes to grain rotation and subdivision producing grain refinement and modification of crystallographic texture of the material that can improve the properties of the sheet during subsequent plastic deformation process^{13,14}. Al alloy strips can exhibit high formability if they are produced via the shear deformation¹⁵. The possibility of generating shear textures across the whole volume of the strip if the shear deformation associated with rolling is strong enough to deliver the shear strain to the centre of the strip. The asymmetric rolled strip exhibited uniform microstructures across the thickness direction, in contrast to the conventionally rolled strip, and a strength comparable to or exceeding that of the commercial Al alloy strip commonly in use.

Cryorolling is a simple low-temperature processing route that requires a relatively lower load to induce severe strain for producing the sub-microcrystalline structural features in materials. The method using rolling under liquid nitrogen temperature has been widely used to improve the materials properties^{16–22}. The cryorolling may be easily adapted for large-scale industrial applications of nanostructured materials¹⁶. Wang et al¹⁷ described a thermomechanical treatment of Cu that results in a bimodal grain size distribution, with micro meter-sized grains embedded inside a matrix of nanocrystalline and ultrafine grains. The matrix grains impart high strength, as expected from an extrapolation of the Hall-Petch relationship. Meanwhile, the inhomogeneous microstructure induces strain hardening mechanisms that stabilize the tensile deformation, leading to a high tensile ductility elongation to failure, and 30% uniform elongation. Cryorolling has been identified as one of the potential routes to produce bulk ultrafine grained Al alloys from its bulk alloys¹⁸. The microstructure and mechanical properties of a precipitation hardening Al-Cu alloy subjected to cryorolling, low temperature annealing and ageing treatments were studied by Rangaraju et al²⁰. Under optimal processing conditions, ultrafine grained microstructure with improved tensile strength and good ductility was obtained. Due to the suppression of dynamic recovery during cryorolling both the tensile strength and yield strength were considerably increased. Moreover, the cryorolling



process offers other advantages, such as, lower required plastic deformations, simple processing procedures and ability to produce continuously long length product, as compared to other severe plastic deformation processes²¹.

Recent developments in the field of both asymmetric rolling and cryorolling processes have led to a renewed interest in improvement of the grain refinement of materials. However, no research has been found that surveyed materials using the methods together. In this paper, the nanostructural Al 1050 sheet was produced by asymmetric cryorolling technique. Meanwhile, the mechanical properties of Al 1050 under different ratios upper and down rolling velocities (RUDV) were studied. When the RUDVs increase from 1.1 to 1.4, both the strength and the ductility of Al 1050 sheets increase.

Results

Fig. 1 shows the mechanical properties of the rolled Al 1050 sheet. In Fig. 1(b), with increasing the RUDVs, both the yield stresses and tensile stresses of the sheets increase. The tensile stress is 160 MPa when the RUDV is 1.1, which reaches 196 MPa for RUDV 1.4 with an increase of 22.3%. Meanwhile, with increasing strength, the ductile also increases slightly as shown in Fig. 1 (c).

Fig. 2 shows the TEM graph of the samples after asymmetric cryorolling process. Compared Fig. 2 (b) and (c), the grain size in Al 1050 sheet with the RUDV 1.1 is much larger than that with the RUDV 1.4. After rolling process, the grain size is 360 nm when the RUDV is 1.1, and the grain size is 211 nm when the RUDV is 1.4.

Eq. (1) shows the Hall-Petch relationship,

$$\sigma_r = \sigma_i + k_y D^{-1/2} \quad (1)$$

where k_y is Petch parameter, D is grain size. Sato et al²³ analyzed the Hall-Petch relationship of Al 1050 in friction stir welds of equal channel samples. The extrapolated value for a boundary-free condition and slope of the Hall-Petch equation give values of $H_0 \approx 18$ Hv, $k_H \approx 19$ Hv, which means the $\sigma_i \approx 58$ MPa, and $k_y \approx 62$ MPa $\mu\text{m}^{-1/2}$ (σ_i and k_y equal 3~3.5 times of H_0 and k_H respectively). According to Eq (1), the calculated tensile stress for RUDV of 1.1 is 161 MPa, and that for RUDV of 1.4 is 193 MPa. They are in agreement with the measured values.

Discussion

The suppression of dynamic recovery during deformation at extremely low temperatures is expected to preserve a high density of defects generated by deformation²⁴. With decreasing the deformation temperature, the strength of Aluminum alloys generally increases. Moreno-Valle et al²⁵ studied the strength properties of an Al 6061 alloy at room and cryogenic temperatures using high pressure torsion. A decrease of the testing temperature results in improved strength of ultrafine grain materials, increased strain hardening coefficient, and enhanced elongation to failure. Su et al²⁶ compared the strength of commercial-purity aluminum using ECAP at room temperature and that at cryogenic temperature with liquid nitrogen cooling. The cryogenic temperature ECAPed samples had higher hardness values than the room temperature ECAPed samples. The increased hardness of the cryogenic temperature ECAPed samples can be attributed to the existence of bulk mono and divacancies in these samples which are the major vacancy-type defects that can work as dislocations pinning centers and induce hardening.

A dislocation cell structure²⁷ is assumed to form during deformation, which consist of dislocation cell wall (ρ_c), statistical dislocation density (ρ_{ws}) and geometrically necessary dislocation density (ρ_{wg}). When the resolved shear strain rate ($\dot{\gamma}$) across the cell walls and cell interior are equal, ρ_c , ρ_{ws} and ρ_{wg} are governed by the following equations,

$$\rho_c = \gamma \left(\alpha^* \frac{1}{\sqrt{3}b} \sqrt{\rho_{ws} + \rho_{wg}} - \beta^* \frac{6}{bd(1-f)^{1/3}} - k_0 \left(\frac{\dot{\gamma}}{\dot{\gamma}_0} \right)^{-1/n} \rho_c \right) \quad (2)$$

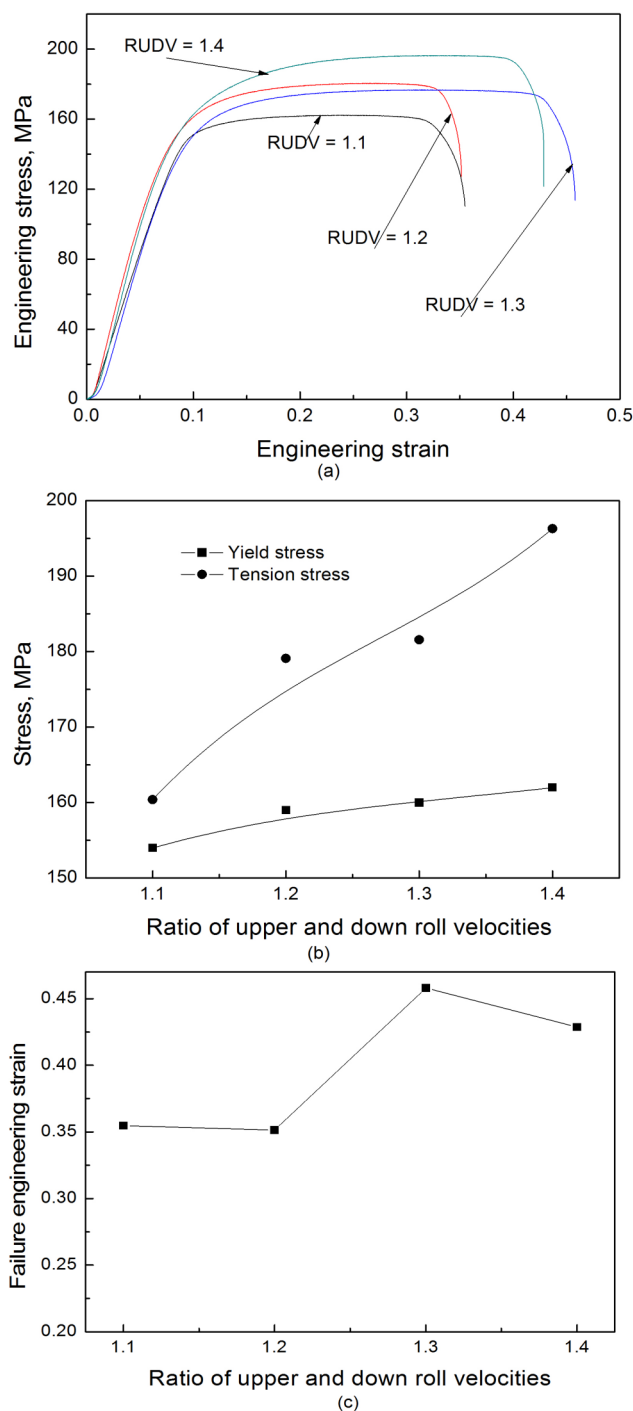


Figure 1 | Curve of engineering stress-strain (a), tensile and yield stress (b) and failure strain (c) of Al 1050 under various ratios of upper and down rolling velocities.

$$\rho_{ws} = \gamma \left(\beta^* \frac{\sqrt{3}(1-f)}{fb} \sqrt{\rho_{ws} + \rho_{wg}} + (1-\xi)\beta^* \frac{6(1-f)^{2/3}}{bdf} - k_0 \left(\frac{\dot{\gamma}}{\dot{\gamma}_0} \right)^{-1/n} \rho_{ws} \right) \quad (3)$$

$$\rho_{wg} = \gamma \xi \beta^* \frac{6(1-f)^{2/3}}{bdf} \quad (4)$$

where α^* , β^* are dislocation evolution rate control parameters for the material; n is a temperature sensitivity parameter, $n = \frac{B}{T}$, for pure

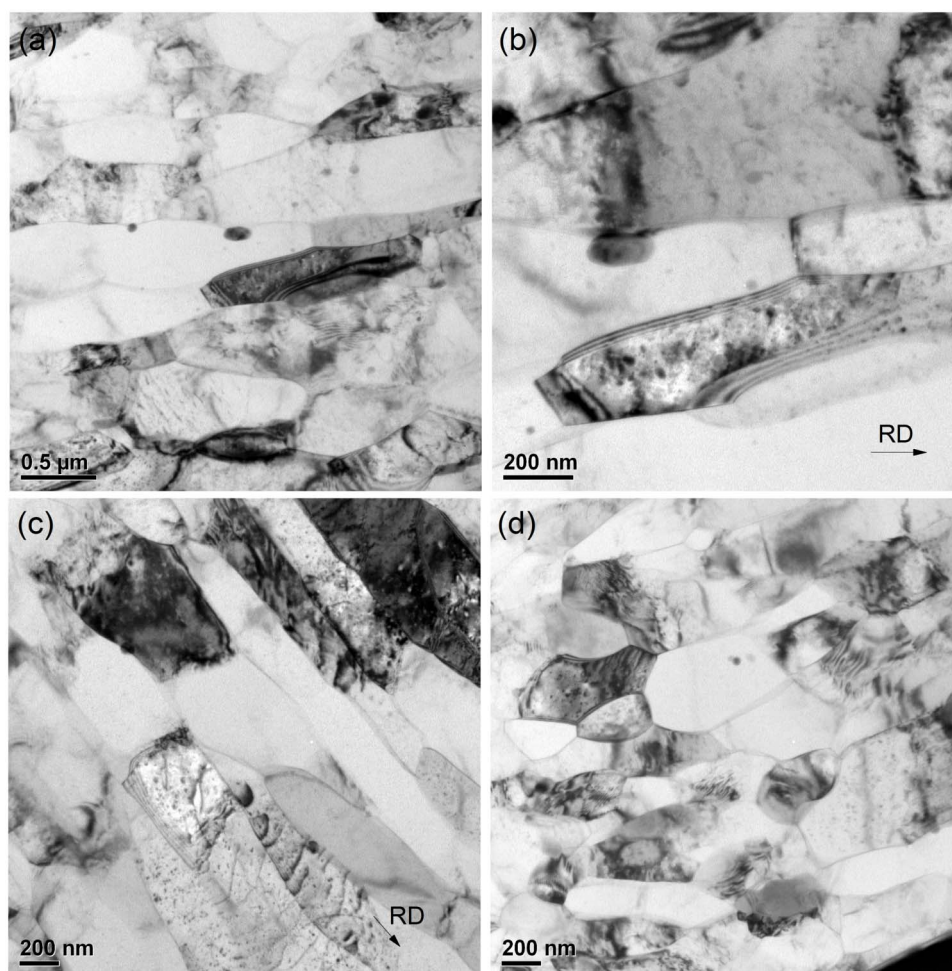


Figure 2 | TEM micrograph of Al1050 after rolling with ratio of upper and down rolling velocities 1.1 for RD (a), (b) and 1.4 for RD(c) and TD(d) (RD - rolling direction; TD - transverse direction).

aluminum, $B = 14900 \text{ K}^{28}$, T is temperature; f is the volume fraction of the dislocation cell wall; b is the magnitude of the Burgers vector of the material; k_0 is the dislocation annihilation rate parameter,

$$k_0 = 1.334 \times 10^{-5} T^2 - 1.176 \times 10^{-3} T + 6.14 \quad (5)$$

From the Eq (5), when the temperature is higher than the liquid nitrogen temperature, the dislocation density will increase with decreasing the temperature. Meanwhile, from the Eqs (2)~(4), with increasing shear strain, the dislocation density will also increase.

Grain growth rate(v), migration rate, and the driving force on the role of grain boundaries per unit area are on the following relationship²⁹:

$$v = mP \quad (6)$$

where, m is the grain boundary mobility, P is the driving force of grain boundary movement, which can be related with the shear modulus(μ) and dislocation density (ρ) of the material, as shown as follows,

$$P = 0.5\rho\mu b^2 \quad (7)$$

From Eqs (6) and (7), with increasing the dislocation density, the grains of materials will be refined. It is reported that shear deformation plays a critical role in the grain refinement of materials processed by ECAPs as well as by asymmetric rolling³⁰. The simple shear deformation through the thickness of the sheet is absolutely essential for property improvement, as well as the techniques ECAP, HPT, and asymmetric rolling. Very small recrystallized grains were

observed in the adiabatic shear bands in metal when they were heavily deformed at high strain rates. Hines³¹ et al observed the recrystallized grains with 100–200 nm diameters within the shear bands of copper. Zuo et al³² observed the extremely fine grains with size of 500 nm in pure aluminum when asymmetric rolling process was used. With improved asymmetric rolling, the ability of grain refinement of asymmetric rolling is greatly improved.

This study, sheets are rolled between rolls that are rotating at different velocities in asymmetric cryorolling process. During asymmetric rolling, the complete strain state imposed to the strip is a combination of plane strain deformation and of an additional shear component imposed on the rolling plane in the rolling direction¹⁵. The asymmetric rolled strip exhibited uniform microstructures across the thickness direction, in contrast to the conventionally rolled strip, and a strength comparable to or exceeding that of the commercial Al alloy strip commonly in use. Fig. 3 shows the friction force distribution in the rolling deformation zone with increasing the RUDVs. In the normal rolling, the upper and down rolling velocities are the same, $RUDV = 1.0$, there are mainly two zones that are forward zone and backward zone, as shown in Fig. 3(a). With the RUDV larger than 1.0, a shear zone appears in the deformation zone, as shown in Fig. 3(b). It is easy to understand that when the RUDV is larger than a certain value, the whole deformation zone will become shear zone, as shown in Fig. 3(c). During asymmetric rolling, the strain of sheet is combined by the plain strain and shear strain. With certain reduction ratio, the plain strain is certain. However, the shear strain in deformation zone will increase with increasing the RUDVs.

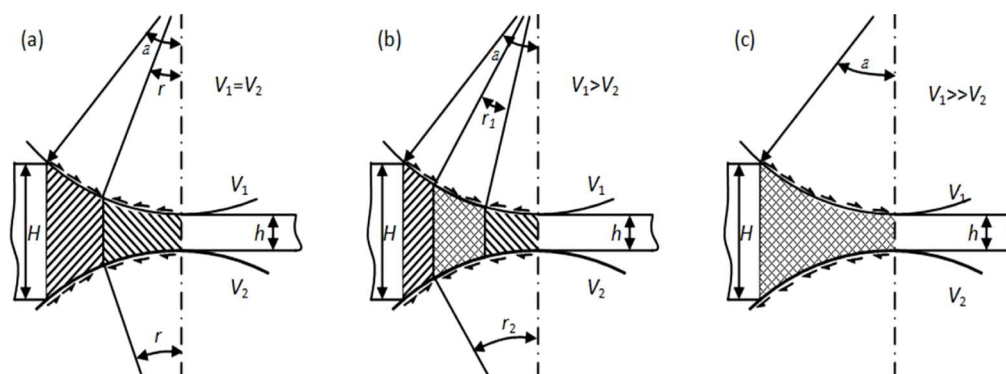


Figure 3 | Friction force distribution in the deformation zone for normal rolling (a), asymmetric rolling for low RUDV (b), and asymmetric rolling for high RUDV (c).

For that, from Eqs (2)~(4), the dislocation density increases with increasing the RUDVs.

A model has been developed for calculation of the uniform elongation of polycrystalline metals as a function of grain size by Liu³³, as shown in Eq (8).

$$\varepsilon_u = \varepsilon_y + \frac{\hat{\sigma}_{s\infty}(1 - \Lambda_s/D)^{0.5}}{\theta_0} \ln \left(\frac{\hat{\sigma}_{s\infty}(1 - \Lambda_s/D)^{0.5} + \theta_0}{\hat{\sigma}_{s\infty}(1 - \Lambda_s/D)^{0.5} + \sigma_y} \right) \quad (8)$$

where ε_u is the uniform strain; the ε_y is the elastic strain; D is grain size; $\hat{\sigma}_{s\infty}$ is overall dislocation stress at steady state as $D = \infty$; Λ_s is the dislocation cell size at steady state, it is a function of temperature and strain rate, but independent on strain and grain size. $\theta_0 = C_1 M^2 \alpha \mu / 2$, C_1 is the probability for a moving dislocation of unit length to be stopped and subsequently stored at an obstacle, M is Taylor orientation factor, α is a constant, μ is shear modulus; σ_y is yield stress. In the model, it suggests that the occurrence of the instability of plasticity in ultrafine grained materials results from the lack of dislocation storages caused by the high density of high angle grain boundaries. In Fig. 2(a), there are many high angle grain boundaries when the RUDV is 1.1. However, the number of high angle grain boundaries is much less when the RUDV is 1.4, as shown in Fig. 2(c). Marker lines were scratched on the polished specimen surfaces using a nano-indenter to measure grain boundary sliding offsets during deformation by Liu and Ma³⁴, which indicated that the grain boundary sliding contribution to the strain exceeded 50% and increased with increases in strain and temperature. Therefore, the high angle grain boundaries in the samples for RUDV of 1.1 should result in its lower ductility compared with that for RUDV of 1.4. Roumina et al¹⁵ also found that the Al alloy strips exhibit high formability when they are produced via the shear deformation.

The asymmetric cryorolling is first time used to produce nanostructural Al 1050 sheets. When the ratio of upper and down rolling velocities is 1.4, the Al 1050 is of grain size with 211 nm, which is much smaller than that obtain by traditional asymmetric rolling with 500 nm. Both the strength and ductility of Al 1050 materials increase with the ratio of upper and down rolling velocities from 1.1 to 1.4. When the ratio of upper and down rolling velocities is 1.4, the tensile stress reaches 196 MPa which is larger by 22.3% than that for the ratio of upper and down rolling velocities of 1.1.

Methods

The commercial 1050 Al alloy was used in this study. It was heat treated at 456°C for 1h before rolling. Asymmetric cryorolling process was employed to produce Al 1050 sheets with size of 1.45 mm × 60 mm × 200 mm under several of ratios of upper and down rolling velocities (RUDV). The RUDVs are 1.1, 1.2, 1.3, and 1.4 separately. Asymmetric cryorolling was performed by dipping the sheets into liquid nitrogen for at least 8 min before each rolling pass. The sheets were rolled to about 0.17 mm after seven rolling passes.

For the tensile tests, the rolled samples were machined into the ASTM subsized specimens with 25 mm gauge length. Uniaxial tensile tests were conducted with an initial strain rate of $1.0 \times 10^{-3} \text{ s}^{-1}$ on an INSTRON machine operating at a constant crosshead speed.

Meanwhile, following asymmetric cryorolling, a FEI xT Nova Nanolab 200 Dualbeam workstation, which combines a focused ion beam and a field emission scanning electron microscope (FIB/SEM), was used to prepare thin-foil specimens from the Al sheets for further TEM observation. The electron beam was used to locate the region of interest on the sample surface, just like that in SEM. The FIB column forms an energetic beam of gallium ions, which scans over the sample surface for imaging as well as ion milling. This system is equipped with an in-situ platinum deposition system, which provides the localized protection on the top surface against the ion beam damage. The typical dimensions of TEM specimens are $15 \mu\text{m} \times 5 \mu\text{m} \times 0.1 \mu\text{m}$. During the FIB milling, an accelerating voltage of 30 kV and high ion beam currents, e.g. 5 nA, were used for rough cutting, and lower beam currents of 1 nA to 0.1 nA were used for polishing both sides of the thin membrane. The electron transparent specimens were then placed on the standard carbon film Cu grid with the ex-situ lift-out method. A Philips CM200 field emission gun transmission electron microscope (FEGTEM) equipped with a Bruker energy dispersive X-ray spectroscopy (EDAX) system was used to investigate the detailed microstructure operating at an accelerating voltage of 200 kV.

- Loucif, A., Figueiredo, R. B., Baudin, T., Brisset, F. & Langdon, T. G. Microstructural evolution in an Al-6061 alloy processed by high-pressure torsion. *Mater. Sci. Eng. A* **527**, 4864-4869 (2010).
- Guo, X., Remennik, S., Xu, C. & Shechtman, D. Development of Mg-6.0%Zn-1.0%Y-0.6%Ce-0.6%Zr magnesium alloy and its microstructural evolution during processing. *Mater. Sci. Eng. A* **473**, 266-273 (2008).
- Kim, J. K., Jeong, H. G., Hong, S. I., Kim, Y. S. & Kim, W. I. Effect of aging treatment on heavily deformed microstructure of a 6061 aluminum alloy after equal channel angular pressing. *Scripta Mater* **45**, 901-907 (2001).
- Lee, S. H., Saito, Y., Sakai, T. & Utsunomiya, H. Microstructures and mechanical properties of 6061 aluminum alloy processed by accumulative roll-bonding. *Mater. Sci. Eng. A* **325**, 228-235 (2002).
- Rezaei, M. R., Toroghinejad, M. R. & Ashrafizadeh, F. Effects of ARB and ageing processes on mechanical properties and microstructure of 6061 aluminum alloy. *J. Mater. Process. Technol* **211**, 1184-1190 (2011).
- Pandey, S. C. et al. A theoretical and experimental evaluation of repetitive corrugation and straightening, Application to Al-Cu and Al-Cu-Sc alloys. *Mater. Sci. Eng. A* **534**, 282-287 (2012).
- Lee, J. W. & Park, J. J. Numerical and experimental investigations of constrained groove pressing and rolling for grain refinement. *J. Mater. Process. Technol* **130**, 208-213 (2002).
- Rusz, S. et al. SEM EBSD and TEM structure studies of a-brass after severe plastic deformation using equal channel rolling followed by groove pressing. *Solid State Phenomena* **186**, 94-97 (2012).
- Kawalek, A. The theoretical and experimental analysis of the effect of asymmetrical rolling on the value of unit pressure. *J. Mater. Process. Technol* **157-158**, 531-535 (2004).
- Kawalek, A., Dyja, H., Mroz, S. & Knapinski, M. Effect of plate asymmetric rolling parameters on the change of the total unit pressure of roll. *Metalurgija* **50**, 163-166 (2011).
- Ji, Y. H. & Park, J. J. Development of severe plastic deformation by various asymmetric rolling processes. *Mater. Sci. Eng. A* **499**, 14-17 (2009).
- Minh, T. N., Sidor, J., Petrov, R. & Kestens, L. A. I. Texture evolution during asymmetrical warm rolling and subsequent annealing of electrical steel. *Mater. Sci. Forum* **702-703**, 758-761 (2012).
- Lee, J. K. & Lee, D. N. Texture control and grain refinement of AA1050 Al alloy sheets by asymmetric rolling. *Int. J. Mech. Sci* **50**(5), 869-887 (2008).



14. Simoes, F., Sousa, R., Gracio, J., Barlat, F. & Yoon, J. W. Effect of asymmetrical rolling and annealing the mechanical response of an 1050-O sheet. *Int. J. Mater. Forming* **2**, 891–894 (2009).
15. Roumina, R. & Sinclair, C. W. Deformation geometry and through-thickness strain gradients in asymmetric rolling. *Metal. Mater. Trans. A* **39**, 2495–2503 (2008).
16. Zhao, Y. H., Liao, X. Z., Cheng, S., Ma, E. & Zhu, Y. T. Simultaneously increasing the ductility and strength of nanostructured alloys. *Adv. Mater* **18**, 2280–2283 (2006).
17. Wang, Y. M., Chen, M. W., Zhou, F. H. & Ma, E. High tensile ductility in a nanostructured metal. *Nature* **419**(31), 912–915 (2002).
18. Sushanta, K. P. & Jayaganthan, R. Effect of ageing on microstructure and mechanical properties of bulk, cryorolled, and room temperature rolled Al 7075 alloy. *J. Alloy. Comp* **509**, 9609–9616 (2011).
19. Shanmugasundaram, T., Murty, B. S. & Subramanya, S. V. Development of ultrafine grained high strength Al-Cu alloy by cryorolling. *Scripta Mater* **54**, 2013–2017 (2006).
20. Rangaraju, N., Raghuram, T., Krishna, B. V., Prasad Rao, K. & Venugopal, P. Effect of cryo-rolling and annealing on microstructure and properties of commercially pure aluminium. *Mater. Sci. Eng. A* **398**, 246–251 (2005).
21. Zhu, Y. T. & Liao, X. Z. Nanostructured metals, retaining ductility. *Nature Mater* **3**, 351–352 (2004).
22. Nageswara rao, P. & Jayaganthan, R. Effects of warm rolling and ageing after cryogenic rolling on mechanical properties and microstructure of Al 6061 alloy. *Mater. Des* **39**, 226–233 (2012).
23. Sato, Y. S., Urata, M., Kokawa, H. & Ikeda, K. Hall-Petch relationship in friction stir welds of equal channel angular-pressed aluminium alloys. *Mater. Sci. Eng. A* **354**, 298–305 (2003).
24. Gang, U. G., Lee, S. H. & Nam, W. J. The evolution of microstructure and mechanical properties of a 5052 aluminium alloy by the application of cryogenic rolling and warm rolling. *Mater. Trans* **50**, 82–86 (2009).
25. Moreno-Valle, E. C., Sabirov, I., Perez-Prado, M. T., Yu Murashkin, M., Bobruk, E. V. & Valiev, R. Z. Effect of the grain refinement via severe plastic deformation on strength properties and deformation behavior of an Al6061 alloy at room and cryogenic temperatures. *Mater. Let* **65**, 2917–2919 (2011).
26. Su, L. H. *et al.* Study of vacancy-type defects by positron annihilation in ultrafine-grained aluminum severely deformed at room and cryogenic temperatures. *Acta Mater* **60**, 4218–4228 (2012).
27. Ding, H., Shen, N. & Shin, Y. Predictive modeling of grain refinement during multi-pass cold rolling. *J. Mater. Process. Technol* **212**, 1003–1013 (2012).
28. Baik, S. C., Estrin, Y., Kim, H. S. & Hellming R. J. Dislocation density-based modeling of deformation behavior of aluminum under equal channel angular pressing. *Mater. Sci. Eng. A* **351**, 86–97 (2003).
29. Hallberg, H., Wallin, M. & Ristinmaa, M. Simulation of discontinuous dynamic recrystallization in pure Cu using a probabilistic cellular automaton. *Comp. Mater. Sci* **49**, 25–34 (2010).
30. Kim, W. J., Lee, J. B., Kim, W. Y., Jeong, H. T. & Jeong, H. G. Microstructure and mechanical properties of Mg-Al-Zn sheets severely deformed by asymmetrical rolling. *Scripta Mater* **56**, 309–312 (2007).
31. Hines, J. A. & Vecchio, K. S. Recrystallization kinetics with adiabatic shear bands. *Acta Mater* **45**, 635–649 (1997).
32. Zuo, F. Q., Jiang, J. H., Shan, A. D., Fang, J. M. & Zhang, X. Y. Shear deformation and grain refinement in pure Al by asymmetric rolling. *T. Nonfer. Metal. Soc. China* **18**, 774–777 (2008).
33. Liu, W. J. Modelling the dependence of uniform elongation on grain size. *Mater. Sci. Forum* **539–543**, 2576–2581 (2007).
34. Liu, F. C. & Ma, Z. Y. Contribution of grain boundary sliding in low-temperature superplasticity of ultrafine-grained aluminum alloys. *Scripta Mater* **62**, 125–128 (2010).

Acknowledgements

The authors gratefully acknowledge the financial supports from the National Natural Science Foundation of China through 51105071, the Doctorate Foundation of the Ministry of Education of China through the Grant. 20090042120005, and the Vice-Chancellor's Fellowship Grant at University of Wollongong. The authors also want to thanks Dr. Hongyan WU, Xiangkun SUN, Delin TANG, in Northeastern University, Shenyang.

Author contributions

YH conceived the study. YH, LC, TK, LX and KC wrote the main manuscript text. YH, LX, SY and KC conducted the experiments. YH, LC, TK, LX, YQ analyzed the data. All authors reviewed the manuscript.

Additional information

Competing financial interests: The authors declare no competing financial interests.

License: This work is licensed under a Creative Commons Attribution-NonCommercial-ShareAlike 3.0 Unported License. To view a copy of this license, visit <http://creativecommons.org/licenses/by-nc-sa/3.0/>

How to cite this article: YU, H. *et al.* Asymmetric cryorolling for fabrication of nanostructural aluminum sheets. *Sci. Rep.* **2**, 772; DOI:10.1038/srep00772 (2012).